

**Hydrogen-Bonded Organic Frameworks**

 International Edition: DOI: 10.1002/anie.201911861  
 German Edition: DOI: 10.1002/ange.201911861

# Microporosity of a Guanidinium Organodisulfonate Hydrogen-Bonded Framework

Ivana Brekalo, David E. Deliz, Leonard J. Barbour, Michael D. Ward, Tomislav Frišćić,\* and K. Travis Holman\*

**Abstract:** Guanidinium organosulfonates (GSs) are a large and well-explored archetypal family of hydrogen-bonded organic host frameworks that have, over the past 25 years, been regarded as nonporous. Reported here is the only example to date of a conventionally microporous GS host phase, namely guanidinium 1,4-benzenedisulfonate (*p*-G<sub>2</sub>BDS). *p*-G<sub>2</sub>BDS is obtained from its acetone solvate, AcMe@G<sub>2</sub>BDS, by single-crystal-to-single-crystal (SC-SC) desolvation, and exhibits a Type I low-temperature/pressure N<sub>2</sub> sorption isotherm ( $S_{A_{BET}} = 408.7(2) \text{ m}^2 \text{ g}^{-1}$ , 77 K). SC-SC sorption of N<sub>2</sub>, CO<sub>2</sub>, Xe, and AcMe by *p*-G<sub>2</sub>BDS is explored under various conditions and X-ray diffraction provides a measurement of the high-pressure, room temperature Xe and CO<sub>2</sub> sorption isotherms. Though *p*-G<sub>2</sub>BDS is formally metastable relative to the “collapsed”, nonporous polymorph, *np*-G<sub>2</sub>BDS, a sample of *p*-G<sub>2</sub>BDS survived for almost two decades under ambient conditions. *np*-G<sub>2</sub>BDS reverts to *z*CO<sub>2</sub>@*p*-G<sub>2</sub>BDS or *y*Xe@*p*-G<sub>2</sub>BDS (*y*, *z* = variable) when pressure of CO<sub>2</sub> or Xe, respectively, is applied.

Since their introduction in 1994,<sup>[1]</sup> guanidinium organosulfonate (GS) compounds have become one of the paramount successes in crystal engineering.<sup>[2,3]</sup> This class of compounds is represented by more than 500 crystalline members, with two- (2D) or three-dimensional (3D) frameworks in which 2D hydrogen-bonded GS sheets persist owing to multiple charge-assisted N–H⋯O hydrogen bonds (e.g. the quasi-hexagonal motif in Figure 1b). The most studied GS

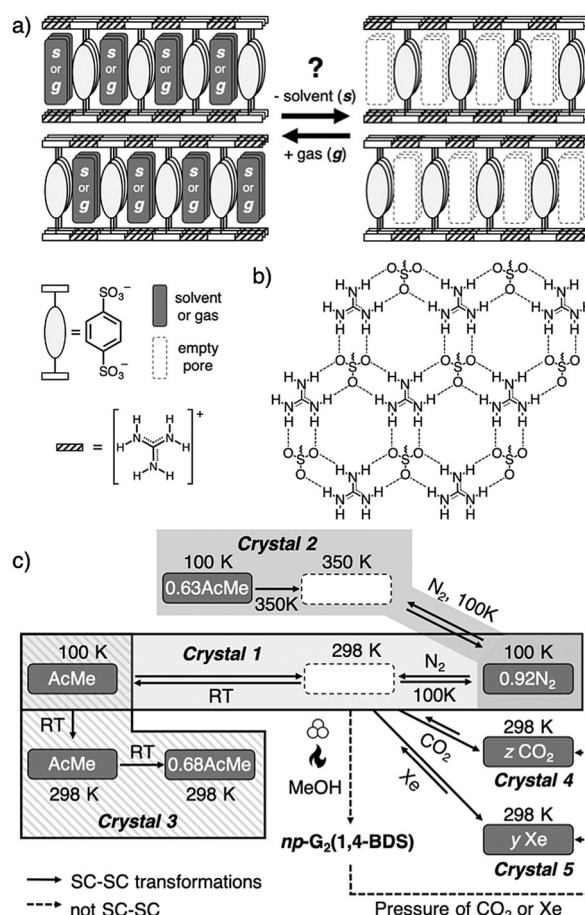


**Figure 1.** a) Schematic representation of SC-SC desorption/sorption of solvents (s) or gases (g) from/into the bilayer crystal form of porous G<sub>2</sub>BDS. b) The quasi-hexagonal hydrogen-bonded 2D network of guanidinium cations and sulfonate anions. c) Schematic summary of the SC-SC experiments and form behavior described herein.

compounds are guanidinium organodisulfonates due to their reliable propensity to adopt topologically diverse, low-density frameworks that are predisposed to include a variety of guests.<sup>[4]</sup> The structural diversity in this family of materials stems from the pliability of these sheets and the ability of the sulfonate organic groups to project to either side of a sheet and form various architectures (e.g. 2D bilayer, 3D brick, 3D zig-zag, etc.) that enable accommodation of differently sized, shaped, and functionalized compounds as guests. In this manner, GS inclusion compounds have been used for small-molecule separations,<sup>[5]</sup> pheromone or luminophore binding,<sup>[6,7]</sup> structural analysis of target guests,<sup>[8]</sup> the design of

[\*] I. Brekalo, D. E. Deliz, Prof. K. T. Holman  
 Department of Chemistry, Georgetown University (GU)  
 37th and O Street NW, 20057 Washington, DC (USA)  
 E-mail: kth7@georgetown.edu  
 Homepage: <http://www.holmanchemistry.net/>

Prof. T. Frišćić  
 Department of Chemistry, McGill University  
 Montreal, Quebec, H3A 0B8 (Canada)  
 E-mail: tomislav.frisic@mcgill.ca  
 Homepage: <https://friscic.research.mcgill.ca/>

Prof. L. J. Barbour  
 Department of Chemistry and Polymer Science  
 University of Stellenbosch  
 Matieland, 7600 (South Africa)

Prof. M. D. Ward  
 Molecular Design Institute, Department of Chemistry  
 New York University  
 100 Washington Square East, 10003 New York (USA)

Supporting information and the ORCID identification number(s) for the author(s) of this article can be found under:  
<https://doi.org/10.1002/anie.201911861>.

nonlinear optical materials,<sup>[9]</sup> the confinement of reactive species,<sup>[10]</sup> chiral discrimination,<sup>[11]</sup> etc.<sup>[2,3]</sup>

Recently, the acronym “HOF” has been coined to describe and name Hydrogen-bonded Organic Framework materials that exhibit persistent porosity.<sup>[12]</sup> Unfortunately, the acronym obscures the myriad of hydrogen-bonded frameworks, such as GS hosts, that preceded the use of this term. To distinguish HOFs that exhibit porosity from those for which porosity has not (perhaps, yet) been established, in our view it is imperative to include the descriptor for the porous ones, that is, *p*-HOFs (*p*=porous). *p*-HOFs and other porous molecular solids<sup>[13,14]</sup> have garnered much interest in recent years as they offer several advantages compared to 2D and 3D covalently connected microporous materials (e.g., zeolites, carbons, metal–organic and covalent–organic frameworks, intrinsically porous polymers). For example, their solubility enables solution processing (assembly/disassembly). Additionally, porous molecular solids derived from shape-persistent building blocks can be among the most chemically and thermally stable porous materials; some are essentially incollapsible, as their most thermodynamically stable crystalline form is intrinsically porous.<sup>[15–18]</sup> Of the porous molecular solids family, *p*-HOFs are of particular interest as they are amenable to structural design.<sup>[19,20]</sup>

Given the extraordinary propensity of GS compounds to form 2D and 3D frameworks that can be occupied by a myriad of guests, it is perhaps surprising that conventional porosity in this class of materials has not yet been formally demonstrated, likely because the focus has been primarily on their inclusion behavior. This is also remarkable given the recent demonstration of porosity in related alkyl ammonium sulfonates.<sup>[21]</sup> Indeed, the frameworks of GS inclusion compounds are generally thought to “collapse” upon guest removal and few such guest-free structures are known.<sup>[3]</sup> Of the 210 reported guanidinium organodisulfonate structures in the Cambridge Structural Database, only five are guest-free, exhibiting appreciable empty space ( $\geq 25 \text{ \AA}^3$ ), and only one of those compounds<sup>[22]</sup> has been demonstrated to also include guests, albeit in different topologies. There are, however, a few reports of GS compounds exhibiting behavior related to porosity, including single-crystal-to-single-crystal (SC-SC) exchange of included solvents,<sup>[23,24]</sup> SC-SC dehydration,<sup>[10]</sup> and even a report of supposed porosity.<sup>[25]</sup> Nevertheless, the “burden of proof”<sup>[26]</sup> (demonstration of an open, empty structure that can be reversibly permeated by guests) has never been met. We report here unequivocal evidence of an evacuated, open, conventionally microporous phase of a quintessential GS compound, guanidinium 1,4-benzenedisulfonate (**G<sub>2</sub>(1,4-BDS)** or **G<sub>2</sub>BDS**, Figure 1), that reversibly sorbs gases. The porous phase (*p*-**G<sub>2</sub>BDS**) is found to be metastable relative to its “collapsed” and nonporous crystalline polymorph (*np*-**G<sub>2</sub>BDS**), yet a nearly two-decades-old sample of **G<sub>2</sub>BDS** was found intact as the open, porous form. Moreover, we show that the collapsed form can readily be returned to the porous form by application and release of gas pressure. This work places the long-known GS host framework compounds squarely into the family of contemporary *p*-HOFs, thereby broadening the potential applications of these materials to gas separation/storage, amphidynamic materials,<sup>[27]</sup> etc.

Some of us have previously reported that **G<sub>2</sub>BDS** can crystallize in several topologically distinct forms, depending on the guest.<sup>[4]</sup> Of these, the bilayer structure was targeted for study due to its relative rigidity and because it offers the smallest volume for inclusion of guests, suggesting that it may yield a kinetically and thermodynamically stable porous crystal form. The bilayer guest@**G<sub>2</sub>BDS** structure consists of pairs of the typical quasi-hexagonal 2D hydrogen-bonded sheets connected via aryl struts such that all the struts of each sheet project nearly orthogonally from the same side of the sheet (a topology with all organic groups “up” or all “down”, Figure 1a,b). The pillars leave space for guest molecules within the bilayers, which stack in 3D via ionic interactions. Precipitation of **G<sub>2</sub>BDS** from methanol by vapor diffusion of small antisolvents (e.g., THF,<sup>[4]</sup> acetone (AcMe)) gives bilayer-type solvates. The AcMe@**G<sub>2</sub>BDS** solvate was chosen for study as the high volatility and low surface tension of acetone suggested the material would be amenable to evacuation under mild conditions.<sup>[28]</sup> Indeed, AcMe@**G<sub>2</sub>BDS** crystals desolvate fully at room temperature (RT, SI-2.1.2.) within a day, or within minutes at 120 °C. In fact, obtaining a fully occupied AcMe@**G<sub>2</sub>BDS** structure requires rapid transfer of single crystals from the mother liquor to the 100 K variable-temperature N<sub>2</sub> stream (VTN<sub>2</sub>S), whereas exposure of the crystals to air for even a couple of minutes during mounting resulted in structures that appeared to be only partially solvated. As the majority of those crystals seemed to retain single crystallinity, we sought to formally establish the SC-SC nature of the desolvation process and characterize the partially solvated and empty, porous *p*-**G<sub>2</sub>BDS** phases by monitoring several crystals by single-crystal X-ray diffraction (SCXRD).

A freshly grown crystal of AcMe@**G<sub>2</sub>BDS** (*Crystal 1*) was quickly mounted in the VTN<sub>2</sub>S at 100 K. X-ray analysis revealed that the triclinic crystal adopts a bilayer architecture that is similar to that of the previously reported THF@**G<sub>2</sub>BDS** solvate, with inversion-disordered acetone molecules residing in the cavities (Figure 2a,b). When the same crystal was allowed to warm to RT, the crystal proved to be the fully desolvated *p*-**G<sub>2</sub>BDS** phase, adopting a higher symmetry monoclinic setting. The bilayer architecture is retained in *p*-**G<sub>2</sub>BDS**, however, and it is otherwise geometrically very similar to the 100 K AcMe@**G<sub>2</sub>BDS** phase, but the aryl struts were found to be highly—and almost certainly dynamically—disordered. SQUEEZE<sup>[29]</sup> analysis ( $1e^-/\text{G}_2\text{BDS}$ ) suggested that the crystal had completely lost its solvent (Figure 2c). The *p*-**G<sub>2</sub>BDS** structure exhibits a significant solvent-accessible void volume (static: 34 %, continuous 2D pore network, or dynamic: 17 %, 0D pores; SI-2.2.2.2.). The formal porosity of *p*-**G<sub>2</sub>BDS** became further apparent when *Crystal 1* was slowly cooled back to 100 K under the VTN<sub>2</sub>S. Again, no loss of single crystallinity was observed. Structural analysis revealed that the cooled *p*-**G<sub>2</sub>BDS** crystal remained as the monoclinic bilayer structure (Figure 2d), but the aryl struts were found to be disordered over only two, nearly superimposable positions. Significant residual electron density within the pores suggests that the cavities at 100 K are largely occupied by N<sub>2</sub>, which was modeled over two positions as 0.92N<sub>2</sub>@**G<sub>2</sub>BDS**.

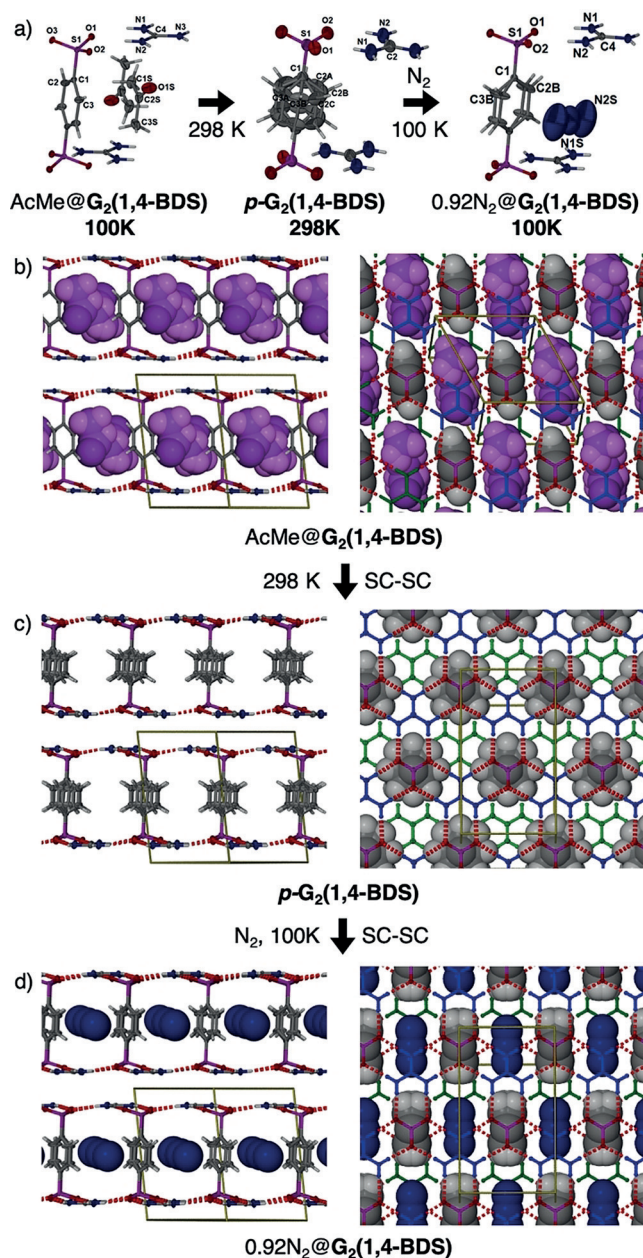


**Figure 2.** SC-SC experiments on *Crystal 1*: a) Thermal ellipsoid plots (50% probability) of  $\text{AcMe}@G_2\text{BDS}$  (100 K), which desolvates at 298 K to give empty  $p\text{-}G_2\text{BDS}$ , and then absorbs dinitrogen to give  $0.92N_2@G_2\text{BDS}$  at 100 K. View down the  $[1\bar{1}0]$  (left) and  $[001]$  (right) directions of the crystal structures of b)  $\text{AcMe}@G_2\text{BDS}$ , c)  $p\text{-}G_2\text{BDS}$ , and d)  $0.92N_2@G_2\text{BDS}$ . Guests (and aryl pillars in the images on the right) are depicted at 80% van der Waals radii.

A second crystal of  $\text{AcMe}@G_2\text{BDS}$  (*Crystal 2*) was more slowly mounted into the 100 K  $\text{VTN}_2\text{S}$ , resulting in the structure of a partial solvate,  $0.63\text{AcMe}@G_2\text{BDS}$ . The framework structure of  $0.63\text{AcMe}@G_2\text{BDS}$  is more similar to  $0.92N_2@G_2\text{BDS}$  than fully solvated  $\text{AcMe}@G_2\text{BDS}$ , except that partially occupied  $\text{AcMe}$  molecules clearly reside in the pores at positions nearly identical to those in  $\text{AcMe}@G_2\text{BDS}$ . Warming the crystal to 350 K (SI-2.2.3.2.) resulted in a  $p\text{-}G_2\text{BDS}$  with no residual electron density in the pores ( $0e^-/\text{cell}$  by SQUEEZE).

In an attempt to slow the desolvation process and determine the RT structure of  $\text{AcMe}@G_2\text{BDS}$ , another crystal of  $\text{AcMe}@G_2\text{BDS}$  (*Crystal 3*) was coated with epoxy glue. The 100 K structure proved it to be the triclinic, fully occupied  $\text{AcMe}@G_2\text{BDS}$ . *Crystal 3* was then warmed to RT and structural analysis revealed a monoclinic form of  $\text{AcMe}@G_2\text{BDS}$ . As with  $0.63\text{AcMe}@G_2\text{BDS}$  at 100 K, the aryl struts of  $\text{AcMe}@G_2\text{BDS}$  at RT are disordered over two nearly superimposable positions, but the cavities are fully occupied by acetone (modelled over two positions). Cooling *Crystal 3* again to 100 K yields the triclinic  $\text{AcMe}@G_2\text{BDS}$  form. Thus, cycling  $\text{AcMe}@G_2\text{BDS}$  between RT and 100 K induces a reversible monoclinic-to-triclinic phase transition due to freezing out the slight disorder of the aryl struts. There is otherwise almost no change in structure; considered in equal settings (SI-2.2.4.2.), the unit cells of the triclinic (100 K) and monoclinic (RT) forms of  $\text{AcMe}@G_2\text{BDS}$  do not differ by more than  $\pm 1.9\%$  in any parameter. Similarly, the RT lattice dimensions of  $\text{AcMe}@G_2\text{BDS}$  are within 1% of those of  $p\text{-}G_2\text{BDS}$ , except for a 2.5% decrease in the  $\beta$  angle that allows differentiation of the occupied  $\text{AcMe}@G_2\text{BDS}$  and empty  $p\text{-}G_2\text{BDS}$  phases by PXRD (Figure S9).

*Crystal 3* was then cycled between RT and 100 K until a partially desolvated structure (monoclinic,  $0.68\text{AcMe}@G_2\text{BDS}$ ), was obtained at RT. The RT framework structure of  $0.68\text{AcMe}@G_2\text{BDS}$  resembles  $p\text{-}G_2\text{BDS}$ , with aryl rings disordered over multiple positions, yet the pores remain partially occupied by acetone. Finally, a crystal of  $p\text{-}G_2\text{BDS}$  taken from the oven ( $120^\circ\text{C}$ ) was placed into acetone for about one minute and then analyzed by SCXRD at 100 K. The obtained structure—redundant with the fully occupied  $\text{AcMe}@G_2\text{BDS}$  form—demonstrates the reversibility of the SC-SC (de)solvation process.

The crystallographic results clearly establish the existence of the empty,  $p\text{-}G_2\text{BDS}$  bilayer phase and its permeability to acetone and dinitrogen. The degree of aryl strut disorder observed for RT  $x\text{AcMe}@G_2\text{BDS}$  structures suggests that permeation of  $\text{AcMe}$  in/out of  $G_2\text{BDS}$  at RT occurs concurrently with turnstile-like rotation of the aryl struts. The turnstile mechanism also rationalizes how acetone molecules can leave the  $\text{AcMe}@G_2\text{BDS}$  material easily at RT, without significant deformation of the framework structure, despite the fact that  $\text{AcMe}$  resides in seemingly isolated cavities and not in continuous pores (SI-2.2.2.).

Bulk  $p\text{-}G_2\text{BDS}$  was prepared by drying  $\text{AcMe}@G_2\text{BDS}$  in an oven at  $120^\circ\text{C}$ , and was characterized by PXRD, NMR, TGA, DSC, and porosity experiments (SI-2.1.3., SI-2.5.1.).  $p\text{-}G_2\text{BDS}$  is formally ultramicroporous (SI-2.3.) and exhibits fully reversible Type I gas sorption isotherms (no hysteresis), with the amount of gas absorbed per  $G_2\text{BDS}$  at  $\approx 1$  bar equal to  $1.77 N_2$  ( $111.5(2) \text{ cm}^3 \text{ g}^{-1}$  (STP), 77 K),  $0.550 \text{ CO}_2$  ( $34.54(7) \text{ cm}^3 \text{ g}^{-1}$  (STP), 298 K), and  $0.756 \text{ Xe}$  ( $47.50(5) \text{ cm}^3 \text{ g}^{-1}$  (STP), 298 K). The  $N_2$  sorption isotherm (Figure 3a) gives a BET surface area of  $408.7(2) \text{ m}^2 \text{ g}^{-1}$  and a pore volume of  $102 \text{ \AA}^3$  per  $G_2\text{BDS}$ , suggesting that the rotation of aryl rings is at least partially hindered by the  $N_2$  guest at 77 K (SI-2.2.2.2.), consistent with the 100 K  $0.92N_2@G_2\text{BDS}$  crystal structure. To explore the high-pressure sorption behavior of  $p\text{-}G_2\text{BDS}$ , we selected two single crystals of  $p\text{-}G_2\text{BDS}$  and mounted

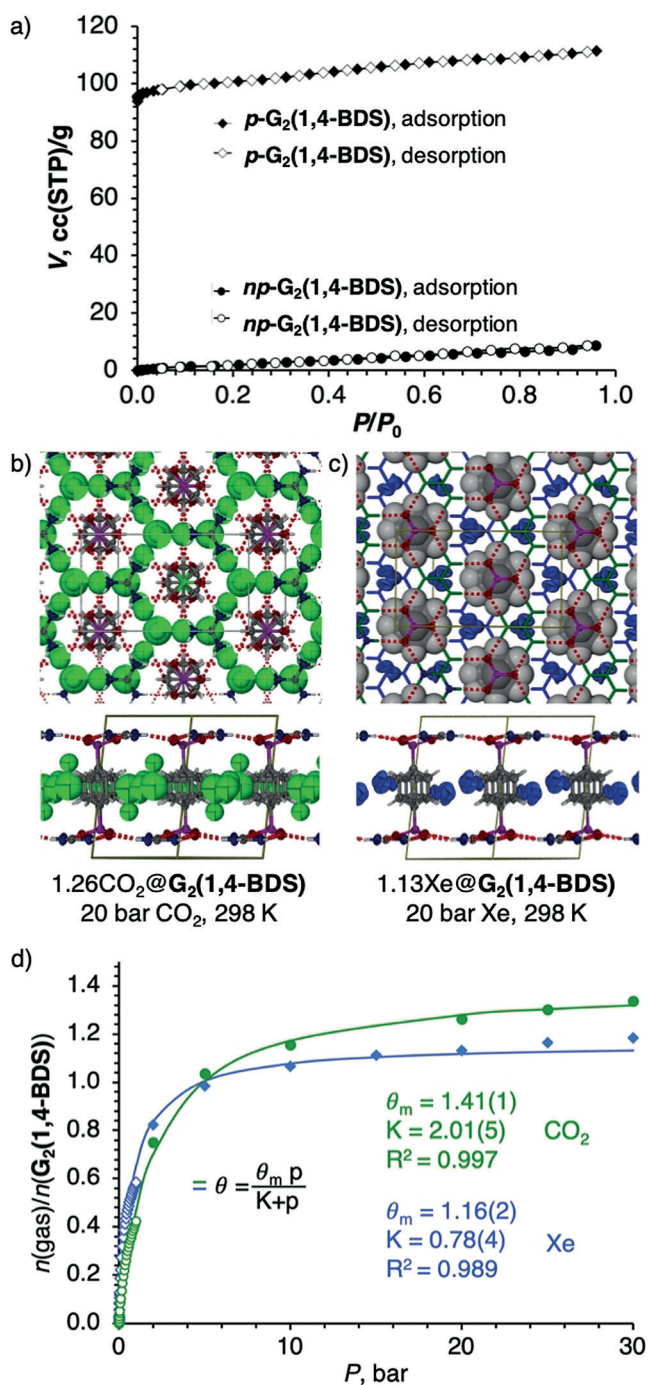


**Figure 3.** a) Low-pressure  $\text{N}_2$  sorption isotherms (77 K) of  $p\text{-G}_2\text{BDS}$  (diamonds) and  $np\text{-G}_2\text{BDS}$  (circles) polymorphs. View down the [001] (top) and [110] (bottom) directions of the crystal structures of b)  $1.26\text{CO}_2@G_2(1,4\text{-BDS})$ , and c)  $1.13\text{Xe}@G_2(1,4\text{-BDS})$ . d)  $\text{CO}_2$  (circles, green) and Xe (diamonds, blue) volumetric (0–1 bar, open) and SCXRD (2–30 bar, filled) isotherms of  $p\text{-G}_2\text{BDS}$  at RT.

them in a variable-pressure gas cell (SI-1.2.).<sup>[30]</sup> The crystals were evacuated and confirmed to be fully empty  $p\text{-G}_2\text{BDS}$  by SCXRD. They were then pressurized with 2, 5, 10, 15,<sup>[31]</sup> 20, 25, and 30 bar of  $\text{CO}_2$  (Crystal 4) or Xe (Crystal 5), and SCXRD data (298 K) were collected at each pressure until equilibrium was established, the electron density analysis

providing high-pressure SCXRD adsorption isotherms (Figure 3 d).

For both the  $\text{CO}_2$ - and Xe-occupied crystals, the framework structure at any given pressure was nearly identical to that in the  $p\text{-G}_2\text{BDS}$  structure (298 K, 1 atm), with the principal difference being an increase in electron density which corresponds to an increasing amount of  $\text{CO}_2$  or Xe guest within the pores as a function of gas pressure (SI-2.4.). Both crystals exhibited Type I sorption isotherms at RT that approach saturation at gas pressures near 30 bar. Moreover, the SCXRD gas-occupancy data well complement the volumetric low-pressure isotherms obtained on microcrystalline  $p\text{-G}_2\text{BDS}$ . The combined RT volumetric (0–1 bar) and SCXRD (2–30 bar) isotherms are shown in Figure 3 d. The data are well modeled by the Langmuir equation, as shown.

The DSC trace of  $p\text{-G}_2\text{BDS}$  exhibits—aside from melting ( $T_0 = 213.6^\circ\text{C}$ ) and recrystallization ( $T_0 = 166.3^\circ\text{C}$ ) peaks—a small exotherm ( $\Delta H = 8.0 \text{ J g}^{-1} = 2.9 \text{ kJ mol}^{-1}$ ,  $T_0 = 181.5^\circ\text{C}$ ) indicative of a phase transformation from  $p\text{-G}_2\text{BDS}$  to what proved to be a “collapsed”, nonporous polymorph,  $np\text{-G}_2\text{BDS}$ . The PXRD pattern (Figure S25) of the sample after DSC (crystallization from melt) showed it to be a mixture of  $p\text{-G}_2\text{BDS}$  (major) and  $np\text{-G}_2\text{BDS}$  (minor), whereas grinding of  $p\text{-G}_2\text{BDS}$  led to conversion of the majority of the sample to  $np\text{-G}_2\text{BDS}$ . Analysis of the ground sample by synchrotron PXRD allowed for structure determination (SI-2.5.3.). Pure  $np\text{-G}_2\text{BDS}$  was eventually prepared by evaporation from methanol, allowing for SCXRD (SI-2.5.2.), DSC (Figure S26), and sorption analysis (Figure 3 a).

Importantly,  $np\text{-G}_2\text{BDS}$  does not adopt the typical quasi-hexagonal hydrogen-bonded network structure. Instead, the framework is collapsed such that each guanidinium cation is bound to five different sulfonate groups via  $\text{N-H}\cdots\text{O}$  bonds (SI-2.5.2.) that collectively appear to be less favorable (slightly longer, and less linear) than those in  $p\text{-G}_2\text{BDS}$ . In addition, the ordered nature of  $np\text{-G}_2\text{BDS}$  suggests that it is less entropically favored than the dynamic  $p\text{-G}_2\text{BDS}$  form. On the other hand,  $np\text{-G}_2\text{BDS}$  ( $\rho = 1.61 \text{ g cm}^{-3}$ ) is considerably more dense than  $p\text{-G}_2\text{BDS}$  ( $\rho = 1.12 \text{ g cm}^{-3}$ ). As a result of the interplay of these effects,  $np\text{-G}_2\text{BDS}$  is the slightly more thermodynamically stable polymorph (in the range of RT– $\approx 185^\circ\text{C}$ ), as evidenced by the observed transformation and the fact that, occasionally, crystals of  $p\text{-G}_2\text{BDS}$  were observed to convert to  $np\text{-G}_2\text{BDS}$  spontaneously under ambient conditions.

Interestingly, despite being metastable relative to  $np\text{-G}_2\text{BDS}$ ,  $p\text{-G}_2\text{BDS}$  exhibits remarkable kinetic stability; porous  $p\text{-G}_2\text{BDS}$  can crystallize from the melt, and single crystals can typically withstand a variety of conditions (gas sorption/evacuation, solvation/desolvation, and heating to at least  $120^\circ\text{C}$ ). In fact, PXRD analysis of an 18-year-old sample of  $G_2\text{BDS}$ —originally prepared by precipitation of  $G_2\text{BDS}$  from MeOH with acetone<sup>[4]</sup> and stored in glass vials under ambient conditions—revealed it to be the phase-pure, porous  $p\text{-G}_2\text{BDS}$  form (Figures S1–S3)! Furthermore, due to the small energy difference between the  $p\text{-G}_2\text{BDS}$  and  $np\text{-G}_2\text{BDS}$ , and demonstrated affinity of the former towards polarizable gases at room temperature, we hypothesized that pressurization of  $np\text{-G}_2\text{BDS}$  with gases could induce a struc-

tural transformation to a gas-occupied *p*-**G<sub>2</sub>BDS** phase similar to that described for other porous molecular solids.<sup>[32]</sup> Indeed, pressurizing *np*-**G<sub>2</sub>BDS** with either 30 bar of CO<sub>2</sub> or 21.5 bar of Xe results in full conversion to the gas-occupied open forms, *z*CO<sub>2</sub>@**G<sub>2</sub>BDS** or *y*Xe@**G<sub>2</sub>BDS** (Figure S31), providing a reliable means to regenerate the *p*-**G<sub>2</sub>BDS** phase after collapse.

In conclusion, we have demonstrated persistent porosity and explored the rich phase behavior and gas sorption characteristics of **G<sub>2</sub>BDS**, one of the simplest members of an archetypal class of hydrogen-bonded frameworks, the guanidinium organodisulfonates. Though *p*-**G<sub>2</sub>BDS** is metastable relative to its nonporous polymorph (*np*-**G<sub>2</sub>BDS**), it can be kinetically stable on a timescale of decades, and thereby formally predates most contemporary examples of *p*-HOFs. Even after collapse, the open *p*-**G<sub>2</sub>BDS** framework can be regenerated from *np*-**G<sub>2</sub>BDS** by simply applying gas pressure. This discovery opens the door for the well-established group of GS frameworks to be used in the fields of porous molecular solids, gas sorption/separations, and as amphidynamic crystals.

### Acknowledgements

This work was supported by the NSF (DMR-1610882). I.B. acknowledges support from GU (Kunin Fellowship), the ICDD (Ludo Frevel Scholarship), and the IUCr (travel grant). We thank Prof. M. Garcia-Garibay for suggesting the study of **G<sub>2</sub>BDS**, and Drs. S. Lapidus and N. Henderson for help with collecting the synchrotron PXRD data and with PXRD structure solution. Use of the Advanced Photon Source at Argonne National Laboratory was supported by the U.S. Department of Energy, Office of Science, Office of Basic Energy Sciences, under Contract No. DE-AC02-06CH11357.

### Conflict of interest

The authors declare no conflict of interest.

**Keywords:** gas sorption · guanidinium sulfonates · hydrogen-bonded organic frameworks · porosity · porous molecular solids

**How to cite:** *Angew. Chem. Int. Ed.* **2020**, *59*, 1997–2002  
*Angew. Chem.* **2020**, *132*, 2013–2018

- [1] V. A. Russell, M. C. Etter, M. D. Ward, *Chem. Mater.* **1994**, *6*, 1206.
- [2] K. T. Holman, A. M. Pivovarov, J. A. Swift, M. D. Ward, *Acc. Chem. Res.* **2001**, *34*, 107.
- [3] T. Adachi, M. D. Ward, *Acc. Chem. Res.* **2016**, *49*, 2669.
- [4] K. T. Holman, S. M. Martin, D. P. Parker, M. D. Ward, *J. Am. Chem. Soc.* **2001**, *123*, 4421.
- [5] A. M. Pivovarov, K. T. Holman, M. D. Ward, *Chem. Mater.* **2001**, *13*, 3018.
- [6] W. C. Xiao, C. H. Hu, M. D. Ward, *Cryst. Growth Des.* **2013**, *13*, 3197.
- [7] M. Handke, T. Adachi, C. Hu, M. D. Ward, *Angew. Chem. Int. Ed.* **2017**, *56*, 14003; *Angew. Chem.* **2017**, *129*, 14191.
- [8] Y. Li, S. Tang, A. Yusov, J. Rose, A. N. Borrforss, C. T. Hu, M. D. Ward, *Nat. Commun.* **2019**, *10*, 4477.
- [9] K. T. Holman, A. M. Pivovarov, M. D. Ward, *Science* **2001**, *294*, 1907.
- [10] a) Y. Liu, M. D. Ward, *Cryst. Growth Des.* **2009**, *9*, 3859; b) Y.-M. Legrand, A. van der Lee, M. Barboiu, *Science* **2010**, *329*, 299.
- [11] R. Custelcean, M. D. Ward, *Cryst. Growth Des.* **2005**, *5*, 2277.
- [12] a) R. B. Lin, Y. He, P. Li, H. Wang, W. Zhou, B. Chen, *Chem. Soc. Rev.* **2019**, *48*, 1362; b) P. Brunet, M. Simard, J. D. Wuest, *J. Am. Chem. Soc.* **1997**, *119*, 2737.
- [13] A. G. Slater, A. I. Cooper, *Science* **2015**, *348*, aaa8075.
- [14] M. Mastalerz, *Chem. Eur. J.* **2012**, *18*, 10082.
- [15] a) A. I. Joseph, S. H. Lapidus, C. M. Kane, K. T. Holman, *Angew. Chem. Int. Ed.* **2015**, *54*, 1471; *Angew. Chem.* **2015**, *127*, 1491; b) A. I. Joseph, G. El-Ayle, C. Boutin, E. Léonce, P. Berthault, K. T. Holman, *Chem. Commun.* **2014**, *50*, 15905; c) C. M. Kane, O. Ugono, L. J. Barbour, K. T. Holman, *Chem. Mater.* **2015**, *27*, 7337; d) C. M. Kane, A. Banisafar, T. P. Dougherty, L. J. Barbour, K. T. Holman, *J. Am. Chem. Soc.* **2016**, *138*, 4377.
- [16] T. Tozawa, J. T. A. Jones, S. I. Swamy, S. Jiang, D. J. Adams, S. Shakespeare, R. Clowes, D. Bradshaw, T. Hasell, S. Y. Chong, et al., *Nat. Mater.* **2009**, *8*, 973.
- [17] M. Mastalerz, M. W. Schneider, I. M. Oppel, O. Presly, *Angew. Chem. Int. Ed.* **2011**, *50*, 1046; *Angew. Chem.* **2011**, *123*, 1078.
- [18] J. L. Atwood, L. J. Barbour, A. Jerga, B. L. Schottel, *Science* **2002**, *298*, 1000.
- [19] J. D. Wuest, *Chem. Commun.* **2005**, 5830.
- [20] A. Pulido, L. Chen, T. Kaczorowski, D. Holden, M. A. Little, S. Y. Chong, B. J. Slater, D. P. McMahon, B. Bonillo, C. J. Stackhouse, A. Stephenson, C. M. Kane, R. Clowes, T. Hasell, A. I. Cooper, G. M. Day, *Nature* **2017**, *543*, 657.
- [21] A. Comotti, S. Bracco, A. Yamamoto, M. Beretta, T. Hirukawa, N. Tohnai, M. Miyata, P. Sozzani, *J. Am. Chem. Soc.* **2014**, *136*, 618–621.
- [22] CSD entry QOWWII represents guest-free guanidinium octanedisulfonate (see ref. [4]), for which three inclusion compounds have also been reported, none of which adopt the architecture of the guest-free compound.
- [23] W. Xiao, C. Hu, M. D. Ward, *J. Am. Chem. Soc.* **2014**, *136*, 14200.
- [24] Y. Li, M. Handke, Y.-S. Chen, A. G. Shtukenberg, C. T. Hu, M. D. Ward, *J. Am. Chem. Soc.* **2018**, *140*, 12915.
- [25] A bilayer phase of guanidinium 1,5-naphthalenedisulfonate (**G<sub>2</sub>NDS**) was reported to be a member of a “new class of porous proton-conductors”: A. Karmakar, R. Illathalappil, B. Anothumakkool, A. Sen, P. Samanta, A. V. Desai, S. Kurungot, S. K. Ghosh, *Angew. Chem. Int. Ed.* **2016**, *55*, 10667; *Angew. Chem.* **2016**, *128*, 10825; The purported porous **G<sub>2</sub>NDS** phase did not, however, show uptake of N<sub>2</sub> (77 K), H<sub>2</sub>, (77 K), or O<sub>2</sub> (195 K) at low temperature/pressure. The PXRD patterns of the **G<sub>2</sub>NDS** phases, including the purported porous **G<sub>2</sub>NDS** phase, indicate the presence of impurities. Moreover, TGA analysis of the purported empty **G<sub>2</sub>NDS** phase revealed a mass loss (4–5%), and the only reported crystal structure was that of an undefined **G<sub>2</sub>NDS** inclusion compound (CSD ref. code: IWOYAW).
- [26] L. J. Barbour, *Chem. Commun.* **2006**, 1163.
- [27] a) M. E. Howe, M. A. Garcia-Garibay, *J. Org. Chem.* **2019**, *84*, 9835; b) A. Comotti, S. Bracco, P. Sozzani, *Acc. Chem. Res.* **2016**, *49*, 1701.
- [28] a) J. E. Mondloch, O. Karagiari, O. K. Farha, J. T. Hupp, *CrystEngComm* **2013**, *15*, 9258; b) J. Ma, A. P. Kalenak, A. G. Wong-Foy, A. J. Matzger, *Angew. Chem. Int. Ed.* **2017**, *56*, 14618; *Angew. Chem.* **2017**, *129*, 14810.
- [29] A. T. Spek, *Acta Crystallogr. Sect. C* **2015**, *71*, 9.
- [30] P. Lama, L. J. Barbour, *J. Am. Chem. Soc.* **2018**, *140*, 2145.

- [31] Data at 15 bar CO<sub>2</sub> is omitted because instrument access issues required an equilibration time that was longer than the time-frame over which the gas-tight nature of the gas cell could be guaranteed.
- [32] a) P. K. Thallapally, B. P. McGrail, H. T. Schaefer, S. J. Dalgarno, J. Tian, J. L. Atwood, *Nat. Mater.* **2008**, *7*, 146; b) J. Tian, P. Thallapally, J. Liu, G. J. Exarhos, J. L. Atwood, *Chem. Commun.* **2011**, *47*, 701; c) P. Sozzani, S. Bracco, A. Comotti, L. Ferretti, R. Simonutti, *Angew. Chem. Int. Ed.* **2005**, *44*, 1816; *Angew. Chem.* **2005**, *117*, 1850.

Manuscript received: September 17, 2019  
Accepted manuscript online: October 29, 2019  
Version of record online: December 6, 2019